

RC-LACE stay report

Implementation of the quasi-3D turbulence scheme within the ALARO Canonical Model Configuration

Mario Hrastinski

Supervised by: Petra Smolíková

25.4-20.5.2022.

CHMI, Prague, Czech Republic

1 Introduction

Turbulence is, on average, a dominant process within the Planetary Boundary Layer (PBL), which controls the exchange of momentum, mass, heat, and moisture between the surface and atmosphere. Its representation, i.e., parameterization, is in most Numerical Weather Prediction (NWP) models based on assumptions strictly valid only for horizontally homogeneous and flat terrain. As such, it only accounts for the vertical turbulence exchange, assuming that horizontal effects are negligible. This approach is suitable for numerical models with a grid spacing of several kilometers and more.

The computational power of current supercomputers enables the launching of operational NWP models at a grid spacing of approximately 1 km or even less. If followed by the improved description of terrain, land cover, and soil properties, this leads to the enhanced representation of processes within PBL. However, this is insufficient in heterogeneous and mountainous complex terrain (MCT) when horizontal grid spacing (Δx) is ≈ 1 km. Recent research indicate the necessity of including 3D processes, like horizontal shear and advection, to improve the representation of Turbulence Kinetic Energy (TKE) in such an environment [1, 2, 3]. Following the approach of [4], [2] have parameterized horizontal shear effects and included them in TKE prognostic equation to improve the representation of turbulence in shear and thermally driven flows at $\Delta x \approx 1$ km. They also stressed the importance of the Horizontal Turbulence Length

Scale (HTLS), fixed to a constant value and proportional to Δx in both cases. Such treatment of HTLS is adopted from Large Eddy Simulation (LES) models and is not appropriate for resolutions of typical NWP models. For this reason, [3] developed more physically-based and variable HTLS dependent on the state of the PBL. Although it seems promising, this HTLS formulation still has to be tested for different cases and locations.

Given that ALARO Canonical Model Configuration (CMC) is already being tested at $\Delta x \leq 1$ km, the above-mentioned quasi-3D approach is a potential upgrade of the existing turbulence scheme and a starting point for its transition to the full 3D. Moreover, it was identified similarly for other CMCs at the 3D physics side meeting of the 2nd ACCORD All Staff Workshop. For this reason, it was decided to devote this research stay to implementation of quasi-3D turbulence scheme described in [2] and [3] into ALARO CMC, as well as to its preliminary validation. The report is organized as follows. The quasi-3D scheme and its implementation are described in Chapter 2. Preliminary results are presented in Chapter 3. The plan for further work and preliminary conclusions are highlighted in Chapter 4.

2 Quasi-3D turbulence scheme and its implementation

2.1 Description of the quasi-3D turbulence scheme

ALARO CMC utilizes the Third Order moments (TOMs) Unified Condensation Accounting N-dependent Solver (for turbulence and diffusion) – TOUCANS scheme to represent vertical diffusion of momentum, heat, and moisture ([5] and [6]). The central part of the scheme is a solver for a pair of prognostic turbulence energies, i.e., TKE and Turbulence Total Energy (TTE):

$$\frac{de_k}{dt} = -g \frac{\partial}{\partial p} \left(\rho K_{e_k} \frac{\partial e_k}{\partial z} \right) + I + II - \frac{e_k^{\frac{3}{2}}}{\tau_k} \quad (1)$$

$$\frac{de_t}{dt} = -g \frac{\partial}{\partial p} \left(\rho K_{e_t} \frac{\partial e_t}{\partial z} \right) + I - \frac{e_t^{\frac{3}{2}}}{\tau_t} \quad (2)$$

where e_k and e_t are TKE and TTE, K_{e_k} and K_{e_t} are turbulent diffusion coefficients for TKE and TTE, while τ_k and τ_t are dissipation time scales for TKE and TTE. I and II denote the

shear production term and buoyancy production/destruction term given by:

$$I = -\overline{u'w'} \frac{\partial \bar{u}}{\partial z} - \overline{v'w'} \frac{\partial \bar{v}}{\partial z} \quad (3)$$

$$II = E_{s_{sL}} \overline{s_{sL}'w'} + E_{q_t} \overline{q_t'w'} \quad (4)$$

where u , v and w are wind components, s_{sL} is static energy and q_t is total moisture. Further, $E_{s_{sL}}$ and E_{q_t} are cloud fraction dependent parameters given by Eq.(21) and Eq.(22) in [6], while products of primed quantities in Eq.(3) and Eq.(4) are turbulent fluxes of momentum, heat, and moisture. Here we also want to emphasize that the role of the term II is twofold and depends on static stability. In statically unstable conditions, it acts as a source of turbulence, and in statically stable conditions as a sink. The other terms in Eq.(1) and Eq.(2) have the following meaning (from left to right): i) total tendency (can be split into local tendency - $\partial e_{k,t}/\partial t$ and advection - $\vec{V} \cdot \nabla e_{k,t}$, where \vec{V} is velocity vector $\vec{V} = u\vec{i} + v\vec{j} + w\vec{k}$), ii) turbulence transport (vertical; note that transport coefficients are different for TKE - K_{e_k} and TTE - K_{e_t}) and iii) dissipation of TKE and TTE.

The quasi-3D scheme is based on adding the horizontal effects to the shear production term (the second term on the right-hand side):

$$I = \underbrace{-\overline{u'w'} \frac{\partial \bar{u}}{\partial z} - \overline{v'w'} \frac{\partial \bar{v}}{\partial z}}_{I_{vert}} - \underbrace{\overline{u'w'} \frac{\partial \bar{u}}{\partial x} - \overline{u'v'} \frac{\partial \bar{u}}{\partial y} - \overline{u'v'} \frac{\partial \bar{v}}{\partial x} - \overline{v'v'} \frac{\partial \bar{v}}{\partial y}}_{I_{horiz}} \quad (5)$$

We follow the work of [2] and [3], who parameterized the horizontal shear production (HSP) with a Smagorinsky type of closure [4]:

$$\frac{\partial}{\partial t} (e_{k,t})_{hshear} = L_H^2 \cdot \left[\left(\frac{\partial u}{\partial x} \right)^2 + \left(\frac{\partial v}{\partial y} \right)^2 + \frac{1}{2} \left(\frac{\partial u}{\partial y} + \frac{\partial v}{\partial x} \right)^2 \right]^{\frac{3}{2}} \quad (6)$$

where L_H is HTLS, Δx is grid spacing and terms in square brackets are zonal and meridional derivatives of mean horizontal wind components. In the initial configuration of the quasi-3D scheme, HTLS is considered constant and proportional to Δx :

$$L_H = c_s \Delta x \quad (7)$$

In the above Eq.(7), c_s is a dimensionless Smagorinsky constant with a value between 0.2 and 0.25. The concept of a single-length scale, proportional to Δx , originates from LES models. The full 3D schemes of such models are designed to treat only small-scale processes. Since these processes are isotropic, it is reasonable to have a single-length scale proportional to Δx . However, the applicability of this concept in NWP models and resolutions of current ALARO CMC configurations is very questionable. For this reason, [3] developed a variable length scale that depends on actual conditions within the PBL. Their length scale (λ) can be expressed as follows:

$$\lambda = U \cdot \tau \quad (8)$$

where U is the velocity scale and τ is corresponding time scale. In practice, the mean horizontal wind speed (W) is applied as a velocity scale. To account for the spatial inhomogeneity and PBL structure, the Lagrangian Integral Time scale (LIT or T_L) is chosen. Finally, the expression for variable HTLS is:

$$L_H^2 = W^2 \cdot T_{L,u} T_{L,v} \quad (9)$$

where time scales in zonal ($T_{L,u}$) and meridional ($T_{L,v}$) directions are computed as follows:

$$T_{L,u} = 0.15 \frac{H_{PBL}}{\sigma_u}, \quad T_{L,v} = 0.15 \frac{H_{PBL}}{\sigma_v} \quad (10)$$

In the above Eq.(10), H_{PBL} is the height of the PBL computed by utilizing the Weak-Capping-Inversion Method (WCIM) [7], while $\sigma_{u,v}$ are zonal and meridional wind variances. In [2] and [3], H_{PBL} computation is based on a method that utilizes bulk Richardson number and has more general applicability than WCIM. Finally, [3] propose to compute $\sigma_{u,v}$ profiles by the indirect method, i.e., from the following surface layer similarity equations:

$$\sigma_u^2 = u_*^2 \left[\left(5 - 4 \frac{z}{H_{PBL}} \right) + \underbrace{0.35 \left(\frac{H_{PBL}}{\kappa L} \right)^{\frac{2}{3}}}_{\text{stat. unstab. cond.}} \right], \quad \sigma_v^2 = 2u_*^2 \left(1 - \frac{z}{H_{PBL}} \right) \quad (11)$$

where u_* is friction velocity, κ is von Karman constant and L is Monin-Obukhov length. The second term in the equation for σ_u is applied only in statically unstable conditions, while the first term and σ_v equation are generally valid.

As discussed in subchapter 2.2, there is a problem with the computation of horizontal wind variances using Eq.(11). For this reason, we seek alternative solutions. The first option is to compute σ_u and σ_v in a more direct way, i.e., from the TOUCANS scheme itself. Within the current TOUCANS code, they are not mutually separated, nor from the σ_w . Hence, some code adaptation is needed. The corresponding expressions can be found in [8]; their Eq.(15a)-(15b). However, when we enter the gray zone of turbulence, it has to be taken into account that these equations represent only the parameterized part of TKE, i.e., the resolved part has to be taken into account. The second option (perhaps faster to implement) is to find an alternative for variable and physically-based HTLS. The simplest option we found in the literature is based on the work of [9]. The authors note that HTLS should depend on properties of the local flow, i.e., on horizontal shear and stretching:

$$L_{H_{shr}} = sW \left[\left(\frac{\partial v}{\partial x} \right)^2 + \left(\frac{\partial u}{\partial y} \right)^2 \right]^{-\frac{1}{2}}, \quad L_{H_{str}} = sW \left[\left(\frac{\partial u}{\partial x} \right)^2 + \left(\frac{\partial v}{\partial y} \right)^2 \right]^{-\frac{1}{2}} \quad (12)$$

where $L_{H_{shr}}$ is HTLS for shear, $L_{H_{str}}$ is HTLS for stretching, and s is the Resolution-Dependent Correction Factor (RDCF) to compensate for the application of finite differences method in the computation horizontal derivatives (in their model). The RDCF was computed as follows:

$$s = \left(\frac{\Delta_0}{\Delta} \right)^\alpha \quad (13)$$

where Δ_0 is the grid spacing at which the model can resolve the most energetic turbulent eddies, Δ is model grid spacing of the actual model, and a is an empirical constant chosen so that the resulting HTLS is comparable to that derived from observations. In our case, the latter will remain as given by [9], i.e., $a=1.45$. However, it is prone to tuning or even dropping, given that we compute derivatives using a different method. Finally, the combined HTLS is derived by averaging the shear and stretching HTLS:

$$L_H = \sqrt{L_{H_{shr}} L_{H_{str}}} \quad (14)$$

Here we note that the averaging operator applied in [9] is different, i.e., we replaced arithmetic averaging with geometric. We did this due to the experience with the vertical turbulent length scale based on TKE. There the impact of the averaging operator has proved minor. However, those operators for which the main length scale vanished with one of the specific scales proved more successful. For arithmetic averaging, it is not the case.

Finally, we note two main differences from [2] and [3] in how we treat the HSP: i) to compute horizontal derivatives, we benefit from the Semi-Lagrangian Horizontal Diffusion (SLHD), and ii) it contributes to other turbulence energy, i.e., TTE.

2.2 Implementation of the quasi-3D turbulence scheme in ALARO CMC

The quasi-3D turbulence scheme was implemented within the CY43t2ag-op1 branch of the code at the CHMI's HPC system. It was coded under the logical switch, while testing showed that implementation does not affect the reference. The subroutines modified during the implementation phase are **acptke.F90** and **aplpar.F90**.

Several computational options within the scheme are related to the HTLS. The first is a basic one and is given by Eq.(7). The second and third options are given by Eq.(12)-(14). They differ in how the HTLS is protected against excessive values, i.e., $L_{H-max2} = \sqrt{\Delta x \cdot \Delta y}$ and $L_{H-max3} = c_s \sqrt{\Delta x \cdot \Delta y}$ respectively.

During the implementation phase of the quasi-3D scheme, we temporarily abandoned the variable HTLS formulation utilized in [3]. The reason for this is the general inapplicability of equations for the computation of variances of horizontal wind, i.e., σ_u and σ_v ; Eq.(11). Note that the applicability is limited to the PBL for purely mathematical reasons. Additionally, equations are based on the surface layer similarity theory and a relatively small sample of observed data. There were several attempts to adapt Eq.(11) for more general use or even to switch off the quasi-3D scheme above the PBL, but none was successful. One of the issues is also the necessary numerical protection of variances against zero values, which may lead to the extremely high value of LIT and HTLS. Unfortunately, the practice has shown that there are typically many such values. In extreme situations, this resulted in the unrealistically high value of TKE and TTE, turbulent diffusion as a whole, and even numerical instability. Since we wanted to be as close as possible to [3], we started to explore other options to compute variances of the horizontal wind. Given that there was a TOUCANS brainstorming event after this stay, we decided to put it on hold for the time being and switched to [9] as an alternative for HTLS formulation.

Additionally, an adaptation of the code was made to have diagnostics of standard TKE and

TTE budget terms (1D scheme), as well as the horizontal shear and HTLS.

3 Results

The quasi-3D scheme was tested for a set of configurations corresponding to [10], i.e., the spatial extent of the domain is approximately the same, with $\Delta x=4, 2,$ and 1 km. Before launching any simulations, the roughness length fields were updated following the procedure developed at CHMI (cf.[11] for details). The case analyzed is adopted from [3]; the 1st of July 2015 thermally driven flow over Alps. The three configurations described above were initialized at 00 UTC from the interpolated INIT file of the CHMI's operational model and run for 72 hours. Time steps that match to $\Delta x=4, 2,$ and 1 km configurations were set to 150, 75, and 40 s. As lateral boundary conditions, we utilized the forecast of the global model ARPEGE, with a coupling frequency of 3 hours. Other relevant settings correspond to those of the current CHMI operational model.

3.1 Analysis of timeseries from different HTLS options

The following text reveals preliminary results obtained with $\Delta x=1\text{km}$ configuration. The impact of the quasi-3D turbulence scheme at coarser horizontal resolution ($\Delta x=2\text{km}$ and $\Delta x=4\text{km}$) is almost negligible, while the performance of constant HTLS worsens as Δx increases (not shown). First of all, it is very encouraging to see that there were no problems with numerical instability with any of the three HTLS options we used. The analysis of spectral norms revealed their gradual development within the first few hours of the forecast and that there are no significant differences between 1D and quasi-3D experiments until the intensity of turbulence reaches its maximum, i.e., until early afternoon. Compared to [3], the HSP values obtained with a constant length scale are too high for the north-facing slope location and even comparable with the Vertical Shear Production (VSP; Fig. 1a-d). Contrary, when variable HTLS is employed, the HSP values become comparable with [3]. Similar to [3], the variable HTLS options show pronounced daily variability, with maxima near sunrise and noon (Fig. 1e-f). However, there is no exact matching. Finally, the TKE values are slightly higher with our variable HTLS formulations (Fig. 1g-h). However, at least they can reproduce a gradual transition towards smaller values after 18UTC at the north-facing slope location. It should be mentioned that our 1D scheme produces higher TKE values than is the case for the COSMO model configuration utilized in [3].

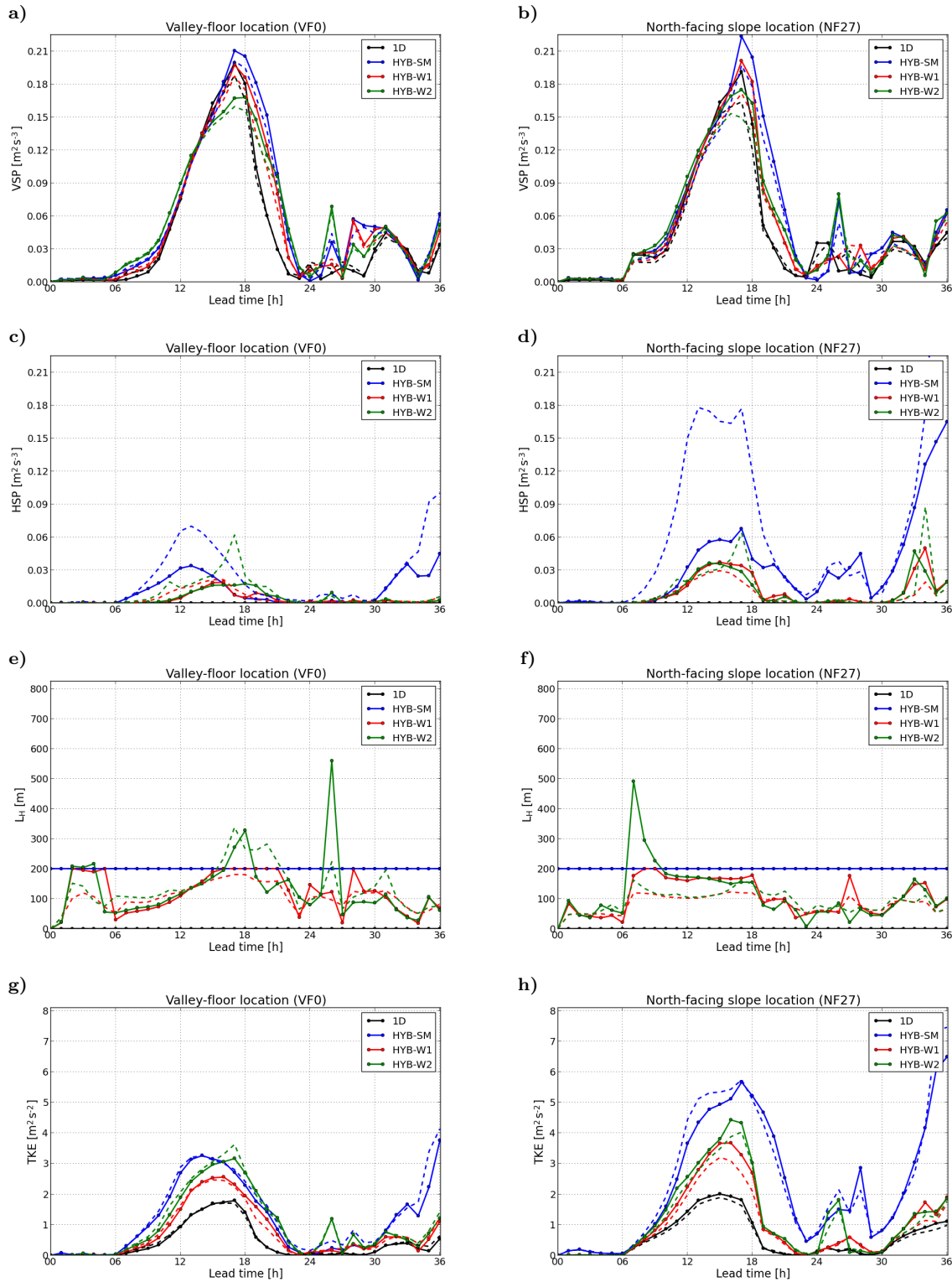


Figure 1: Timeseries of vertical shear production (VSP), horizontal shear production (HSP), horizontal turbulence length scale (L_H), and turbulence kinetic energy (TKE) for valley-floor and north-facing slope location near Innsbruck, Austria, starting from 00 UTC on 1st of July 2015. (1D - 1D scheme, HYB-SM - quasi-3D scheme with L_H from Eq.(7), HYB-W1 - quasi-3D scheme with L_H from Eq.(12)-(14) and upper limit $c_s \cdot \sqrt{\Delta x \cdot \Delta y}$ and HYB-W2 - quasi-3D scheme with L_H from Eq.(12)-(14) and upper limit $\sqrt{\Delta x \cdot \Delta y}$). Full lines denote values from the nearest grid point, while dashed lines denote the mean value of 9 nearest grid points ($\Delta x=1$ km).

3.2 Analysis of vertical profiles from different HTLS options

The vertical profiles of TKE and HSP suggest that turbulence intensity is higher throughout the model column for both valley-floor and north-facing slope locations with the quasi-3D scheme (Fig. 2a and Fig. 2c). Obviously, this is a result of strong HSP near the surface (Fig. 2b and Fig. 2d). The latest variable HTLS option, which allows stronger horizontal mixing, is also able to produce secondary and tertiary maxima in the middle and upper troposphere. That should be a subject of further research as it could provide some benefits for the simulation of jet stream-related turbulence and lateral mixing at the edges of atmospheric fronts.

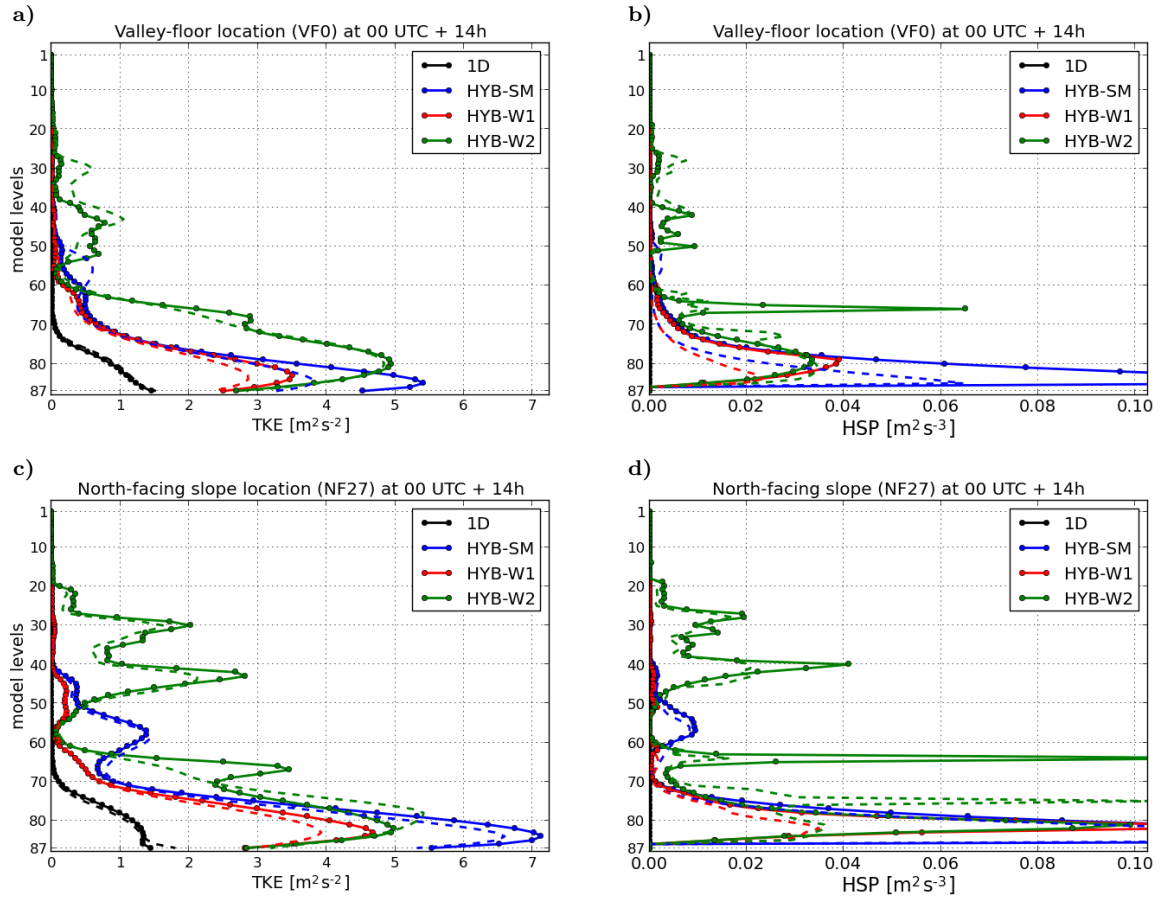


Figure 2: Vertical profile of horizontal shear production (HSP) and turbulence kinetic energy (TKE) for valley-floor and north-facing slope location near Innsbruck, Austria, at 14 UTC on 1st of July 2015. (1D - 1D scheme, HYB-SM - quasi-3D scheme with L_H from Eq.(7), HYB-W1 - quasi-3D scheme with L_H from Eq.(12)-(14) and upper limit $c_s \cdot \sqrt{\Delta x \cdot \Delta y}$ and HYB-W2 - quasi-3D scheme with L_H from Eq.(12)-(14) and upper limit $\sqrt{\Delta x \cdot \Delta y}$). Full lines denote values from the nearest grid point, while dashed lines denote the mean value of 9 nearest grid points ($\Delta x=1$ km).

4 Conclusion and plan for further work

During this stay, we implemented the quasi-3D scheme into the ALARO CMC. The preliminary results indicate that our results are, in principle, consistent with the reference research.

Overall, the turbulence intensity (estimated by TKE) obtained by ALARO CMC is stronger than in [3] for both locations analyzed in this study. Given that this is the case, particularly for the option with constant HTLS, it is likely that our values of horizontal derivatives are higher than those of [3]. Furthermore, the differences might be caused by linking a quasi-3D scheme to TTE and the continuous transition from one energy source to the other. Among other causes of differences, we emphasize: i) different tuning of the turbulence scheme, ii) differences in the representation of the mean and the subgrid orography fields, iii) the strength of applied numerical diffusion, iv) treatment of drag processes and v) the impact of other parameterizations.

In the future, we should perform a more detailed comparison with observations (soundings in particular). Furthermore, the number of cases and locations needs an increase. Given that, in parallel, the quasi-3D scheme is being implemented into AROME CMC, we should exchange knowledge with involved people, do some targeted diagnostics of relevant computational parameters, etc. The HTLS is a crucial quantity for adequate representation of the horizontal effects of turbulence. Hence, one of the main goals is to find its optimal formulation. In that context, the work on LIT computation from TOUCANS-derived turbulence variances will be continued. To make it generally applicable, we should include the impact of resolved turbulence within the gray zone. Further tuning of the variable HTLS formulation implemented during this study is also needed. Finally, the experiments on a domain with $\Delta x=0.5$ km should be conducted.

Acknowledgment: The author wishes to thank to Petra Smolíková for her support and cooperation, as well as to entire ONPP department for their warm welcome and hospitality. This stay is funded by the RC-LACE project.

References

- ¹ D. Arnold, D. Morton, I. Schicker, P. Seibert, M. W. Rotach, K. Horvath, T. Dudhia, T. Satomura, M. Müller, G. Zängl, T. Takemi, S. Serafin, J. Schmidli, and S. Schneider. Issues in high-resolution atmospheric modeling in complex topography—the hircot workshop. *Croat. Meteor. J.*, 47:3–11, 2012.
- ² B. Goger, M. W. Rotach, A. Gohm, O. Fuhrer, I. Stiperski, and A. A. M. Holtslag. The impact of three-dimensional effects on the simulation of turbulence kinetic energy in a major alpine valley. *Bound.-Layer Meteor.*, 168:1–27, 2018.
- ³ Rotach M.W. Gohm A. Stiperski I. Fuhrer O. Goger, B. and G. de Morsier. A new horizontal length scale for a three-dimensional turbulence parameterization in mesoscale atmospheric modeling over highly complex terrain. *J. Appl. Meteorol. Climatol.*, 58:2087–2102, 2019.
- ⁴ J. Smagorinsky. General circulation experiments with the primitive equations. *Mon. Wea. Rev.*, 91:99–164, 1963.
- ⁵ I. Bašták Ďurán, J.F. Geleyn, and F. Váňa. A compact model for the stability dependency of the production-destruction-conversion terms valid for the whole range of richardson numbers. *J. Atmos. Sci.*, 71:3004–3026, 2014.
- ⁶ I. Bašták Ďurán, J.F. Geleyn, F. Váňa, J. Schmidli, and R. Brožková. A turbulence scheme with two prognostic turbulence energies. *J. Atmos. Sci.*, 75:3381–3402, 2018.
- ⁷ K.W. Ayotte, Sullivan P.P., A. Andrén, S.C. Doney, A.A.M. Holtslag, W.G. Large, J.C. McWilliams, C-H. Chin-Hoh Moeng, M.J. Otte, J.J. Tribbia, and J.C. Wyngaard. An evaluation of neutral and convective planetary boundary-layer parameterizations relative to large eddy simulations. *Bound.-Lay. Meteorol.*, 79:131–175, 1996.
- ⁸ Y. Cheng, V. M. Canuto, and A. M. Howard. An improved model for the turbulent pbl. *J. Atmos. Sci.*, 59:1550–1565, 2002.
- ⁹ W. Wang, B. Liu, L. Zhu, Z. Zhang, A. Mehra, and V. Tallapragada. A new horizontal mixing-length formulation for numerical simulations of tropical cyclones. *Wea. Forecasting*, 36:679–695, 2021.
- ¹⁰ M. Hrastinski. Testing the performance of Semi-Lagrangian Horizontal Diffusion (SLHD) at different horizontal resolutions. *RC-LACE stay report*, pages 1–21, 2019.
- ¹¹ J. Mášek. Tools for improving physiography in e923 clim files. https://www.rclace.eu/media/files/ALAR0/alaro1_wd22/presentation_masek_tools.pdf, 2022. Accessed: 2022-09-06.